Supplementary Material

An elastically tethered viscous load imposes a regular gait on the motion of myosin-V

Simulation of the effect of transient force relaxation on a stochastic process

Maria J. Schilstra
Biocomputation Research Group, STRI
University of Hertfordshire
College Lane, Hatfield AL10 9AB, UK
m.j.1.schilstra@herts.ac.uk

Stephen R. Martin
Physical Biochemistry
National Institute for Medical Research
The Ridgeway, Mill Hill, London NW7 1AA, UK
smartin@nimr.mrc.ac.uk

Effect of cargo size on the constant force system (C1)

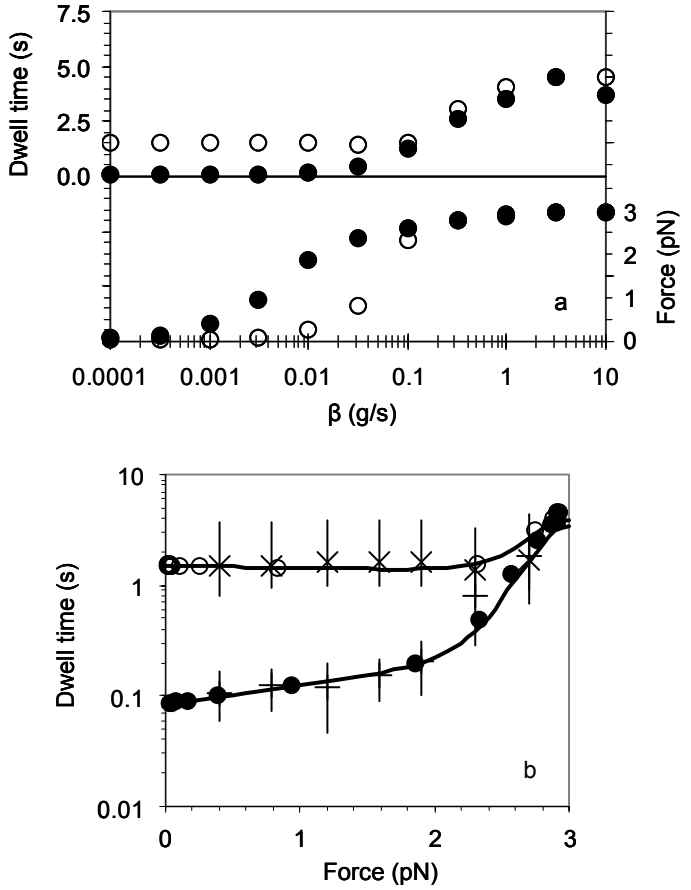

Figure S1. (a) Average dwell times and average force on the motor in a soft-spring system (κ = 0.001 pN/nm) as a function of β, and (b) the same data, plotted as dwell times against force (b). Open symbols: 1 μM ATP, closed symbols: 2 mM ATP. Symbols with error bars: data observed experimentally by Rief et al.(2000) in 1 µM ($\times$) and 2 mM ATP (+). Solid lines: theoretical dependence of forward dwell time τ+ on external force on the motor ($\tau+ = (u_0 + u_1 + w_0 + w_1)/(u_0 \cdot u_1 + w_0 \cdot w_1)$, Kolomeisky and Fisher (2003)). (c) Dwell time distributions for $\beta = 10^{-6}$ (squares), 10^{-5} (circles), and (d) for β = 10-4 kg/s (+) and 10-3 (x). Solid lines indicate the best fit of the data to a double exponential function (see text).

In order to investigate whether motor-spring-cargo combinations in which the force on the motor is essentially constant behave in the same way as myosin-V observed in vitro under constant force, we simulated the behaviour of system C1 (a = 0, b = 0.001 pN/nm, p = 1, so that the stiffness κ is a constant 0.001 pN/nm) for a wide range of loads (β varies from 10^{-8} to 10^{-2} kg/s).

Figure S1a shows that, both at limiting (1 μM) and at saturating (2 mM) ATP concentrations, the mean forward dwell times and the average force on the motor increase with cargo size. Figure S1b shows the same data, but plotted as dwell times against average force. In this graph, we also plotted experimental observations which were obtained using an optical trap in

which the force on the motor was kept constant by means of an electronic feedback system (Rief *et al.* 2000). The solid line indicates the theoretical dependence of forward dwell time on external force on the motor derived by Kolomeisky and Fisher (2003, see Methods). Thus, the behaviour of system **C1** appears to be very similar to the experimental data, and follows the theoretical curve.

Effect of spring stiffness

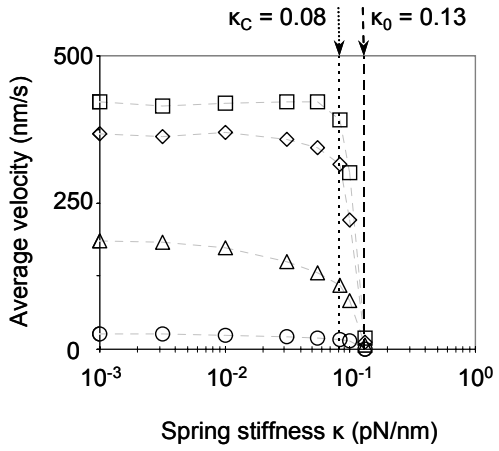

Figure S2. Effect of spring constant κ on the average steady-state motor velocity for various cargo sizes. Values for β (kg/s): squares: 10^{-7}, diamonds: 10^{-6}, triangles: 10^{-5}, circles: 10^{-4}. Vertical lines indicate the values of the critical stiffness, κ_C (dotted line), where the spring's restoring force is equal to the motor stall force when extended over a distance equal to the largest sub-step, and the stalling stiffness, κ_0 (dashed line), beyond which the motor stalls completely.

We also studied the dependence on the spring stiffness κ of the average velocity at different cargo sizes for systems in which κ is constant (a = 0; p = 1).

Figure S2 shows the effect of spring stiffness on average steady state velocity and average force on the motor for a range of cargo sizes. Four types of behaviour can be distinguished.

1) Very soft springs (κ < 0.01 pN/nm) allow the motor to move in an essentially random way at a velocity that can be calculated from the expression for the mean forward and backward dwell times (see main paper, Methods).

2) Springs that are stiffer (0.01 < κ < 0.08 pN/nm), but can still extend by the full step size without producing a force larger than the stall force, F_S, are sufficiently soft to allow the motor to progress relatively unhindered, but do slow it down (with respect to the velocities that are achieved by the very soft spring systems). Motor stepping in these systems is generally more regular and the motion is more uniform than the stepping and motion of the very soft spring systems, and the velocity is determined mostly by the time required for the cargo to move under the restoring force of the spring until it is sufficiently close to the motor (see main paper) .

3) Springs that can only extend by a value between the largest sub-step and the full step size seriously hinder motor progression, even for a small cargo. The 'critical stiffness' constant, κ_C, is the value for κ that, according to Hooke's Law, produces a restoring force equal to F_S when the spring extends by exactly one full step size, here, κ_C = 0.08 pN/nm.

3) Springs that are so stiff that extension by the size of the largest sub-step (22.5 nm) already produces a restoring force greater than the stall force, will be stalled completely by cargo of any size. In this system, the value for κ_0, the stall stiffness, is 0.13 pN/nm.

Effect of cargo size on uniformity and regularity of motion in systems C1 and C2

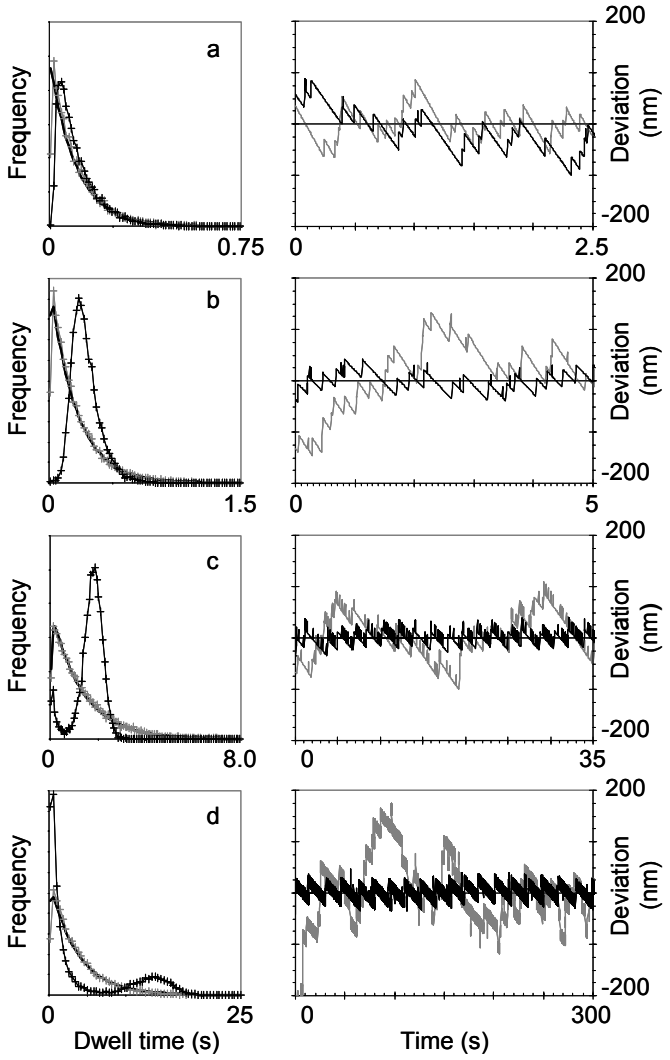

Figure S3. Steady state dwell time distributions (left hand panels) and typical deviation from uniform motion (right hand panels) obtained with system **C1** (grey lines) and system **C2** (black lines) for $\beta = 10^{-6}$ (a), 10^{-5} (b), 10^{-4} (c), and 10^{-3} kg/s (d). Solid black lines (left hand panels) indicate the best fit of the data for system **C1** to a double exponential function ((exp[t/T2] - exp[t/T1])/(T2-T1), Rief *et al.* 2000) with T1 = 0.1, 0.2, 1.3, and 3.6 s, and T2 = 0.0001, 0.005, 0.05, and 0.1 s, for a, b, c, and d, respectively. The significance of the T2 values is low; the shapes of the curves are almost entirely determined by T1. The deviations from uniform motion are normally distributed with a mean of 0 and standard deviations of 50 nm for all cargo sizes in system **C1**, and in system **C2** for $\beta = 10^{-3}$ kg/s, and a mean of 5, and standard deviations of 16 nm (system **C2**, all greater cargo sizes).

At cargo sizes that have a frictional coefficient β that is greater than 10^{-6}, the motion of system **C2** (κ = 0.05 pN/nm) is more regular than that of system **C1** (κ = 0.001 pN/nm). This is borne out by the dwell time distributions in the two systems, shown in Figure S3. The shapes of the histograms for system **C1** indicate that the movement of the motor is essentially random: they are, as expected, satisfactorily described by a double exponential, and reveal a long lifetime that is one or two orders of magnitude larger than the short one. Both lifetimes increase with

β.They are in good agreement with experimentally observed data obtained under constant force (Rief *et al.* 2000), demonstrating the validity of model and simulations. The dwell time distribution at the smallest cargo size (10^{-6} kg/s) for system **C2** is similar to that obtained with system **C1**. However, for larger cargo sizes, the maxima of the distributions are clearly shifted to higher values compared to those for system **C2**, and their shapes are very different. For β = 0.01 g/s, 90% of the steps have dwell times between 0.1 and 0.5 s in system **C1**, and hardly any steps have dwell times below 0.08 s. The mode is at 0.23 s. For β = 10^{-4} and 10^{-3} kg/s, similar modes are observed at 1.9 and 14s, with a spread (full width at half maximum) of 0.9 and 5 s, respectively. Thus, the dwell time distributions for β ≥ 10 mg/s indicate that there is a delay of roughly equal duration between the steps of the stiff spring system, and that stepping is indeed significantly more regular.

The distributions for the two largest cargo sizes are bimodal, for the following reason. In both systems, full backward stepping is rare for cargo with drag coefficients up to about 10^{-5} kg/s, although the backward sub-steps of 22.5 nm are observed more and more frequently when β increases. The forward rates are virtually independent of the force on the motor, so that forward stepping continues to occur at the same frequency when the load increases. However, any 'overambitious' forward step in system **C2** will result in the force on the motor immediately becoming very high, so that such a step will very rapidly be followed by a backward step. Only when the force has reduced enough will one forward sub-step be followed by another forward sub-step. Premature forward steps and their compensating backward steps tend to occur more often when the spring is *almost* sufficiently relaxed, and are usually followed relatively quickly by a new attempt to step forward. Therefore, the distributions in Figure S3c and d also show a number of (exponentially distributed) short dwell times. In addition, full backward steps also shorten the observed average forward stepping dwell time somewhat, as they count as a new full step.

In system **C1**, on the other hand, a forward step may be followed rapidly by several further forward steps, without a very large change in force on the motor. As a result, the motion of system **C2** is more uniform than that of system **C1**, and this effect becomes more pronounced as the load size increases. The right hand panels in Figure S3 illustrate the extent to which the motor deviates from uniform motion for both systems and for various cargo sizes. At β = 10^{-6} kg/s, where the cargo hardly affects motor motion, the deviations from uniformity are the same in both systems. The deviations are normally distributed with a standard deviation of 50 nm, so that excursions of over 100 nm are frequently observed. The distribution of the deviations is the same over the whole range of cargo sizes for system **C1**. The data for system **C2** at the larger cargo sizes (β ≥ 10^{-5} kg/s) are also normally distributed around a mean of 5 nm, and with a standard deviation of only 16 nm. This means that excursions of 50 nm are extremely rare. The non-zero mean reflects the fact that the frequent 'unsuccessful' S1↔S0 oscillations are superposed on the overall trajectory, which is determined by the successful full forward steps (S1→S0→S1).

Effect of contour length on force

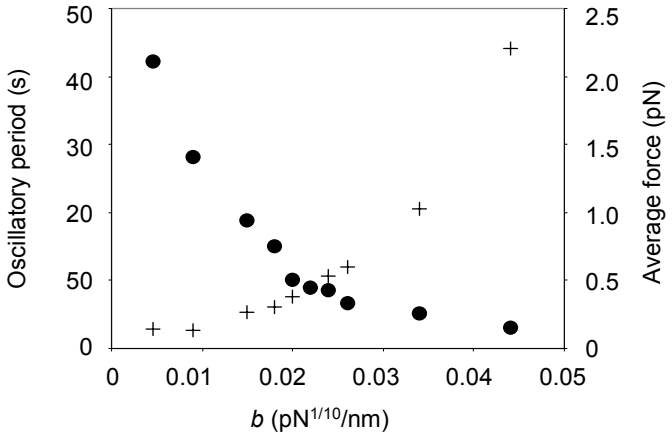

Figure S4. Average force on the motor and duration of oscillatory period as a function of the spring parameter *b*. Plusses (left ordinate): oscillatory periods; circles (right ordinate): average force.

We have investigated the effect of variation in the value of *a* (in the equation $F = ax + (bx)^p$; see main paper), which roughly corresponds to the reciprocal of the contour length, L_C, in the WLC model. The value of *b* was varied between 0.009 $pN^{1/10}$/nm (corresponding to $L_C \approx 140$ nm) to 0.044 ($L_C \approx 29$ nm). The results are shown in Figure S4. The oscillatory period increases from 2.7 (*b* = 0.009) to 44 s (*b* = 0.044), whereas the average force on the motor decreases from 2.1 pN to 0.15 pN.

References

Kolomeisky, A. B. & Fisher, M. E. (2003) A simple kinetic model describes the processivity of myosin-V, *Biophys. J.*, 84, 1642-1650.

Rief, M., Rock, R. S., Mehta, A. D., Mooseker, M. S., Cheney, R. E. & Spudich, J. A. (2000) Myosin-V stepping kinetics: A molecular model for processivity, *PNAS*, 97, 9482-9486.